

# 24 Emission in Wide Band Gap II-VI Semiconductor Compounds with Low Dimensional Structure

X. W. Fan, G. Y. Yu, Y. Yang, D. Z. Shen, J. Y. Zhang,  
Y. C. Liu and Y. M. Lu

*Laboratory of Excited State Processes of Chinese Academy of Sciences, Changchun Institute of Optics, Fine Mechanics and Physics, 140 People Street, Changchun 130022, China*

## 1 INTRODUCTION

Usually the ZnSe-based LD uses a single quantum well or multiple quantum wells as an active layer. It is possible to improve the properties of the LD and other devices, if an asymmetric double quantum wells (ADQWs) structure or a layer with quantum dots is used as an active layer for the LD and other devices. In this paper, our two research works is reported: the first, spontaneous and stimulated emission in ZnCdSe/ZnSe ADQWs; the second, the formation process of CdSe self-assembled quantum dots (SAQDs).

## 2 EMISSION IN ZnCdSe/ZnSe ADQWs

The ZnCdSe/ZnSe ADQWs samples studied were grown on GaAs(100) substrate by LP-MOCVD at 350 °C. The sample structure consists of ten perodes of Zn<sub>0.72</sub>Cd<sub>0.28</sub>Se/ZnSe ADQWs, each period of the ADQWs includes one narrow well (NW), one thin barrier and one wide well (WW), which will be denoted as L<sub>n</sub>/L<sub>b</sub>/L<sub>w</sub>, where L<sub>n</sub>, L<sub>b</sub> and L<sub>w</sub> are the widths of the NW, thin barrier and WW, respectively. Each period of the ADQWs was separated by a 40 nm ZnSe barrier.

## 2.1 Spontaneous Emission

Photoluminescence (PL) spectra were measured under the excited by the 457.9 nm line of a CW Ar<sup>+</sup> laser. The signals were collected by a JY-T800 Raman spectrograph.

Fig. 1 shows the PL spectrum of a 5 nm/3 nm/3 nm ADQWs at 98 K. The emission peaks on the high energy and low energy sides correspond to the  $n=1$  heavy-hole exciton recombination from the NW and WW (Yu *et al.*, 1998), respectively. It is obvious that the emission from the WW dominates the spectrum at this temperature. The main reason that causes the difference in the emission intensity of the NW and WW is the exciton tunneling from the NW to the WW.

Fig. 2 shows the dependence of the integrated intensities of emission from the NW and WW on temperature for this sample. It is obvious that the intensity from the NW ( $I_{NW}$ ) dominates the spectra at low temperature, whereas, with increasing temperature, the intensity from the WW ( $I_{WW}$ ) becomes the dominant one. Another interesting phenomenon is that  $I_{WW}$  increases with increasing temperature in the range of 12-80 K, which is in contrast to usual experimental results and theories. In a usual quantum well structure (Jiang *et al.*, 1988), the emission intensity decreases with increasing temperature throughout the temperature range.

On the basis of the exciton-tunneling and dissociation model, the temperature dependence of the PL intensity  $I$  from the WW and NW can be expressed by the equation.

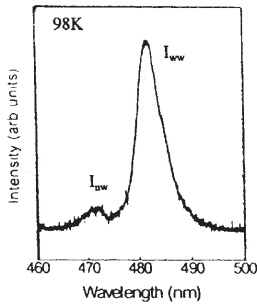


Figure1. The PL Spectrum of the ZnCdSe-ZnSe 5nm/3nm/3nm ADQWs at 98K

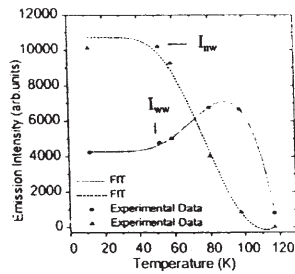


Figure2. The temperature dependence of the emission intensity for the ZnCdSe-ZnSe 5nm/3nm/3nm ADQWs

$$I = \frac{A}{\exp\left(\frac{E_1}{k_B T}\right) - 1} + \frac{A}{1 + c \exp\left(\frac{-E_2}{k_B T}\right)} + D, \quad (1)$$

where A,B,C,D are the constants. The first and second terms on the right-hand side of equation (1) represent the contributions of the exciton tunneling and thermal dissociation to the emission, respectively. By fitting the experimental data for the WW, we obtain  $A > 0$ ,  $E_1 = 32.5$  meV,  $E_2 = 43.2$  meV and  $A > 0$  makes the first term positive, which means that the contribution of the exciton tunneling to the emission from the WW is positive. The value of  $E_1$  is close to the LO-phonon energy of  $\hbar\omega_{LO} \approx 30$  meV and that of  $E_2$  is close to the exciton binding energy of 40 meV for the present Cd fraction. These support our discussion further. On fitting the experimental data for the NW, we obtain  $A < 0$ ,  $E_1 = 31.3$  meV and  $E_2 = 40.4$  meV. It is easy to find that the contribution of the exciton tunneling to the emission from the NW is negative, which implies that the exciton tunneling can decrease the emission from the NW. The value of  $E_1$  and  $E_2$  also support our discussion. The exciton emission both in the NW and in the WW is influenced by two factors: exciton tunneling and thermal dissociation processes. For the NW, the two factors have the same influence on the emission intensity, but for the WW, the influences of the two factors are contrary. The change of the emission intensity is determined by the stronger one.

## 2.2 Stimulated Emission

Photoluminescence and photo-pumped stimulated emission spectra were obtained under the excitation of the 337.1 nm line of a  $N_2$  laser. Two 5 nm/ $L_b$ /3 nm ADQWs samples were studied with the  $L_b = 3$  and 5 nm, respectively. The samples used in the stimulated emission measurement were cleaved to approximately 1 mm wide resonators, and the Fabry-Perot (F-P) cavities were formed by the natural facets of the sample bars.

Fig. 3(a) shows the PL spectra from top surface emission of the sample of a 5 nm/3 nm/3 nm structure and Fig. 3(b) shows the emission from the cleaved edge of this sample. We can see that the emission intensities from different well in Figs. 3(a) and 3(b) change differently with the excitation intensity ( $I_{ex}$ ). Under the condition of surface emission, the emission intensity from the NW ( $I_n$ ) changes faster than that from the WW ( $I_w$ ) with increasing excitation and the emission from the NW

blocked by water and the micromembrane is impermeable to both hydrogen and oxygen. This latter characteristic is important for fuel cell application where the membrane barrier must prevent the cross diffusion of the fuel (i.e., hydrogen) and oxidizer (i.e., oxygen or air) that could lead to a decrease in efficiency.

Nafion is the most popular proton exchange membrane used in the polymer electrolyte membrane fuel cell (PEMFC). Gierke proposed that cations such as proton are transported through the Nafion by traveling from one isolated clusters of hydrated sulfonate groups to another through water filled nanometer-sized channels (Mauritz *et al.*, 1980). This means that water management is critical for the proper operation of a Nafion membrane. Also, the larger pore sizes (~10 nm) of Nafion means that reactant cross over and diffusion of electrode materials must be carefully considered. Membrane shrinkage due to dehydration and its swelling in the presence of methanol and other organic fuel further exacerbate these problems. The polymer membrane also has poorer mechanical strength and lower operating temperature, which severely restrict the operation of a PEM fuel cell. It is therefore attractive to replace the current PEM with an inorganic analog such as zeolite membrane. The HZSM-5 zeolite is one possible candidate.

The ZSM-5 micromembrane shown in Figure 1 was converted into an HZSM-5 micromembrane through ion exchange in an acid solution. Figure 2a shows the proton transport across the hydrated HZSM-5 membrane from a 0.1 N HCl solution to D.D.I. water. The pH of the D.D.I. water decreases as the proton diffuses through the micromembrane under the influence of a concentration gradient until equilibrium is established. Both initial ( $R_0$ ) and average ( $R_{ave}$ ) proton transport rates across the micromembranes can be calculated from these data. Figure 2b displays the plots of  $R_0$  and  $R_{ave}$  as a function of the concentration gradient across the micromembrane. The figure shows that the proton transport rate increases as the concentration gradient increases, but reaches a plateau for  $[H_3O^+]$  concentrations greater than 0.2 M. A maximum proton transport rate of  $1.3 \times 10^{-3} \text{ mole} \cdot \text{m}^{-2} \cdot \text{s}^{-1}$  was obtained from the 5- $\mu\text{m}$  thick HZSM-5 micromembrane.

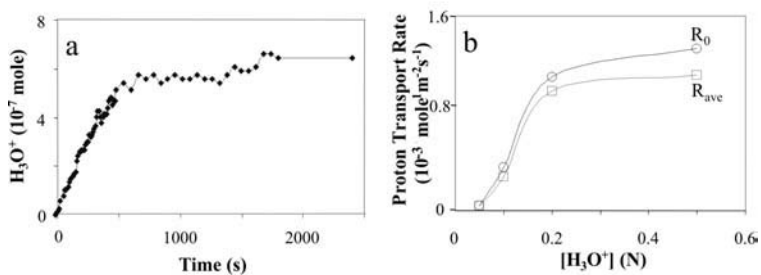


Fig. 2 (a) Moles of proton transported across the zeolite membrane from a 0.1 N HCl solution to deionized water as a function of time. (b) The initial ( $R_0$ ) and average ( $R_{ave}$ ) proton transport rates as a function of the concentration of HCl solution.

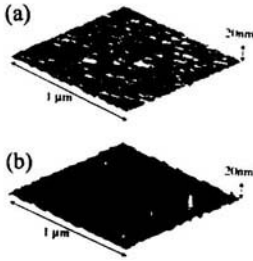


Figure 4. AFM images from the same area on the uncapped CdSe layer surface taken 60(a) and 80(b) min after the growth

Fig. 4 showed the AFM images that were taken as a function of time after the growth. Figs. 4(a) and (b) were taken about 60 and 80 min after the growth of a CdSe layer, respectively. Two kinds of dots were observed on the sample surface. One kind was low dot with high density (a). Another kind was high dot with low density (b), the average height, diameter and density of the dots were 13 nm, 50 nm and 5 dots per  $\mu\text{m}^2$ , respectively. The average diameter-height ratio is about 4, very close to the other II-VI SAQDs under S-K growth mode (Ma *et al.*, 1998, Ko *et al.*, 1997).

The critical thickness for islanding of the CdSe layer on GaAs(100) is about 3ML (Pinardi *et al.*, 1998). In the sample discussed above, only 2 ML of CdSe layer did not reach the critical thickness to form quantum dots by releasing strain. From Figs. 4 (a) to (b), the low lots trended to be grown. These results could be interpreted as the effect of surface diffusion. We considered that surface diffusion could result in parts of the sample surface to reach or exceed the critical thickness, and release strain to form the self-assembled quantum dots. It is concluded that the formation mechanism of CdSe quantum dots below the critical thickness was due to the effect of surface diffusion and releasing strain.

### 3 Conclusions

The spontaneous and stimulated emission in ZnCdSe/ZnSe ADQWs have been studied. The exciton emission both in the NW and WW is influenced by two factors: the exciton tunneling and thermal dissociation. The dependence of the emission intensity on temperature is determined by the stronger one. The carrier tunneling through the thin barrier is conducive to the stimulated emission from the WW. And the lasing threshold in the ADQWs can be lowered by optimizing the structure.

The formation process of CdSe SAQDs on GaAs substrate below the critical thickness was observed by AFM. It revealed that the formation mechanism of CdSe SAQDs below the critical thickness was due to the effect of surface diffusion and strain release.

## ACKNOWLEDGEMENTS

This work was supported by the National Fundamental and Applied Research Project, the National Science Foundation of China (NSFC), the Major Project (No 6989260) of NSFC, the Program of CAS Hundred Talents and the Innovation Project Item of CAS.

## REFERENCES

- Jiang, D. S., Jung, H. and Ploog, K., 1988, Temperature dependence of photoluminescence from GaAs single and multiple quantum well, *J. Appl. Phys.*, 64, pp. 1371.
- Ko, H. C., Park, D. C., Kawakami, Y., Fajita, S., Fujita, Shigeo, 1997, Self-organized CdSe quantum dots onto cleaved GaAs(110) originating from Stranski-Krastanow growth mode, *Appl. Phys. Lett.*, 70, pp. 3278.
- Ma, Z. H., Sun, W. D., Sou, I. K., Wong, G. K. L., 1998, Atomic force microscopy studies of ZnSe self-organized dots fabricated on ZnS/Gap, *Appl. Phys. Lett.*, 73, pp. 1340.
- Pinardi, K., Uma Jain, S. C., Maea, H. E., Van Overstraeten, R., 1998, Critical thickness and strain relaxation in lattice mismatched II-VI semiconductor layers, *J. Appl. Phys.*, 83, pp. 4724.
- Yu, G. Y., Fan, X. W., Zhang, J. Y., Yang, B. J., Shen, D. Z., and Zhao, X. W., 1998, The exciton tunneling in ZnCdSe/ZnSe ADQWs, *J. Electron Mater.*, 27, pp. 1007.